

# Thin disc, thick disc and halo in a simulated galaxy

C. B. Brook,<sup>1,2\*</sup> G. S. Stinson,<sup>3</sup> B. K. Gibson,<sup>2,4,5</sup> D. Kawata,<sup>6</sup> E. L. House,<sup>2</sup>  
M. S. Miranda,<sup>1</sup> A. V. Macciò,<sup>2</sup> K. Pilkington,<sup>2,4,5</sup> R. Roškar,<sup>7</sup> J. Wadsley<sup>8</sup>  
and T. R. Quinn<sup>9</sup>

<sup>1</sup>*Departamento de Física Teórica, Universidad Autónoma de Madrid, Cantoblanco, E-28049 Madrid, Spain*

<sup>2</sup>*Jeremiah Horrocks Institute, University of Central Lancashire, Preston PR1 2HE*

<sup>3</sup>*Max-Planck-Institut für Astronomie, Königstuhl 17, 69117 Heidelberg, Germany*

<sup>4</sup>*Department of Astronomy & Physics, Saint Mary's University, Halifax, Nova Scotia, B3H 3C3, Canada*

<sup>5</sup>*Monash Centre for Astrophysics, Monash University, VIC 3800, Australia*

<sup>6</sup>*Mullard Space Science Laboratory, University College London, Holmbury St. Mary, Dorking, Surrey RH5 6NT*

<sup>7</sup>*Institute for Theoretical Physics, University of Zürich, Winterthurerstrasse 190, CH-8057 Zürich, Switzerland*

<sup>8</sup>*Department of Physics and Astronomy, McMaster University, Hamilton, Ontario, L8S 4M1, Canada*

<sup>9</sup>*Astronomy Department, University of Washington, Box 351580, Seattle, WA 98195-1580, USA*

Accepted 2012 July 18. Received 2012 June 4; in original form 2012 February 26

## ABSTRACT

Within a cosmological hydrodynamical simulation, we form a disc galaxy with sub-components which can be assigned to a thin stellar disc, thick disc and a low-mass stellar halo via a chemical decomposition. The thin- and thick-disc populations so selected are distinct in their ages, kinematics and metallicities. Thin-disc stars are young ( $<6.6$  Gyr), possess low velocity dispersion ( $\sigma_{U,V,W} = 41, 31, 25$  km s<sup>-1</sup>), high [Fe/H] and low [O/Fe]. Conversely, the thick-disc stars are old ( $6.6 < \text{age} < 9.8$  Gyr), lag the thin disc by  $\sim 21$  km s<sup>-1</sup>, possess higher velocity dispersion ( $\sigma_{U,V,W} = 49, 44, 35$  km s<sup>-1</sup>) and have relatively low [Fe/H] and high [O/Fe]. The halo component comprises less than 4 per cent of stars in the ‘solar annulus’ of the simulation, has low metallicity, a velocity ellipsoid defined by  $\sigma_{U,V,W} = 62, 46, 45$  km s<sup>-1</sup> and is formed primarily in situ during an early merger epoch. Gas-rich mergers during this epoch play a major role in fuelling the formation of the old-disc stars (the thick disc). We demonstrate that this is consistent with studies which show that cold accretion is the main source of a disc galaxy’s baryons. Our simulation initially forms a relatively short (scalelength  $\sim 1.7$  kpc at  $z = 1$ ) and kinematically hot disc, primarily from gas accreted during the galaxy’s merger epoch. Far from being a competing formation scenario, we show that migration is crucial for reconciling the short, hot, discs which form at high redshift in  $\Lambda$  cold dark matter, with the properties of the thick disc at  $z = 0$ . The thick disc, as defined by its abundances, maintains its relatively short scalelength at  $z = 0$  (2.31 kpc) compared with the total disc scalelength of 2.73 kpc. The inside-out nature of disc growth is imprinted in the evolution of abundances such that the metal-poor  $\alpha$ -young population has a larger scalelength (4.07 kpc) than the more chemically evolved metal-rich  $\alpha$ -young population (2.74 kpc).

**Key words:** Galaxy: disc – Galaxy: evolution – Galaxy: formation – galaxies: evolution – galaxies: formation.

## 1 INTRODUCTION

The fitting of the vertical distribution by two exponentials has motivated separation of the Milky Way’s disc population into ‘thick’ and ‘thin’ stellar disc components. Such classification has dominated the literature of Galactic structure for the past three decades

(e.g. Gilmore & Reid 1983; Jurić et al. 2008, although see Ivezić et al. 2008; Bovy, Rix & Hogg 2012a). The oldest disc stars in the Milky Way are kinematically hot, show an asymmetric drift (i.e. rotational lag) and have lower metallicities ([Fe/H]) and higher  $\alpha$ -to-iron abundance ratios, with respect to the younger disc stars. Understanding the origin of the stars distributed at the highest vertical scaleheights within the disc – the classical ‘thick disc’ – is an important aspect in our attempts to understand galaxy formation and evolution throughout the Universe, as such thick discs appear

\*E-mail: cbabrook@gmail.com

ubiquitous (e.g. Dalcanton & Bernstein 2002; Yoachim & Dalcanton 2005) and contain the oldest disc stars, born during the earliest formation of discs.

Several models for the formation of such thick stellar discs have been proposed, each of which is able to reproduce one or more of their empirical properties. Despite these partial successes, a singular, universally accepted model has not yet emerged. Such a model needs to answer two fundamental points: (i) the origin of the oldest disc stars and (ii) how these stars attained their present-day properties.

The heating of a pre-existing thin disc due to the accretion of satellite galaxies (Quinn, Hernquist & Fullagar 1993) appears consistent with the hierarchical structure formation of  $\Lambda$  cold dark matter. The signatures of such events are well studied and indeed are able to match vertical profiles of the thick disc (Hayashi & Chiba 2006; Kazantzidis et al. 2008; Villalobos & Helmi 2008; Bekki & Tsujimoto 2011; Qu et al. 2011), including several fine-detailed features (Qu et al. 2011). Such models assume a pre-existing and relatively thin disc. Another model proposes that stars accreted by satellites can be dragged into the plane of a pre-existing disc by dynamical friction (Abadi et al. 2003). Recently, it has been shown that the radial migration of old,  $\alpha$ -enhanced stars from the inner region of the disc to the solar neighbourhood can explain many properties of the thick disc (Schönrich & Binney 2009; Loebman et al. 2011). The ‘popping’ of star clusters (Kroupa 2002; Assmann et al. 2011) or the effects of massive clump formation in unstable gas-rich discs in the early Universe (Noguchi 1999; Bournaud, Elmegreen & Elmegreen 2007; Agertz, Teyssier & Moore 2009; Ceverino, Dekel & Bournaud 2010) may also result in thickening of discs; such scenarios link thickening more to formation processes, rather than to disc heating, per se. Stars may also have been born relatively thick as gas settles into a disc configuration during an early period of gas-rich mergers (Brook et al. 2004b).

It is important to stress that these models are not necessarily mutually exclusive. Indeed, some do not try to explain the formation of the oldest stars, but rather how they were heated, or how they migrated to the solar region. One way to comprehensively probe thick-disc formation is using high-resolution, hydrodynamical, cosmological galaxy formation simulations of Milky Way mass galaxies (Abadi et al. 2003; Scannapieco et al. 2010; Stinson et al. 2010; Kobayashi & Nakasato 2011; Tissera, White & Scannapieco 2011; Doménech-Moral et al. 2012; Martig et al. 2012). These attempts, though, have been hampered by their inability to match several important properties of the Milky Way. In this context, the main problems are (i) the continued formation of overly massive and metal-rich stellar haloes, which makes separation of thick-disc and halo stars more difficult than in the Milky Way where metallicity can be used as an added discriminant, and (ii) the lack of resolution. The first problem has been alleviated by improved feedback (Brook et al. 2004a; Okamoto et al. 2005; Governato et al. 2007; Guedes et al. 2011) but continues to plague even recent simulations (Sales et al. 2012; Scannapieco et al. 2012; Martig et al. 2012). The latter problem is more subtle than just the size of gravitation softening, but relates to the relatively low density and high temperature at which star formation occurs in low-resolution simulations, which prevents thin discs from forming (House et al. 2011).

In this study, we take a complementary approach by examining a disc galaxy simulation of lower mass than the Milky Way, providing us with improved spatial resolution and allowing stars to form at higher densities and lower temperatures. We analyse the simulation first presented in Brook et al. (2012a, B12 hereafter) with a late-type barred galaxy with  $M_{\text{vir}} = 1.9 \times 10^{11} M_{\odot}$ , realized as part of

the MaGICC (Making Galaxies In a Cosmological Context) programme. To re-iterate, this simulation is of a lower mass than that of the Milky Way, and therefore our analysis must be read within this context. That said, we note that the simulated galaxy examined here shares other properties with the Milky Way that we feel make it relevant to analyse in relation to putative theories of thick-disc formation. Although the Milky Way is the only galaxy for which we have detailed abundances and kinematic information, vertically extended ‘thick’ discs appear ubiquitous in nature. Any comparison we make with the Milky Way is not expected to match *exactly*, but is predicated upon the fact that the broad trends of the Milky Way chemodynamics should be generic for relatively massive disc galaxies *which have quiescent merger histories*, in the sense that the last major merger was early in the galaxy’s evolution. There is evidence that the Milky Way had such a quiescent merging history (e.g. Hammer et al. 2007). However, if these assumptions were to be shown to be false, our model would clearly unravel.

The second feature of our study is our chemical decomposition of stars into different galactic sub-components based on abundance patterns. The ability to separate components based purely on their chemical ‘tags’ is at the heart of Galactic archaeology (Freeman & Bland-Hawthorn 2002). A multitude of studies has shown that thin- and thick-disc stars with similar iron abundances ( $[\text{Fe}/\text{H}]$ ) differ in their abundances of  $\alpha$  elements (e.g. Majewski 1993; Fuhrmann 1998; Chiba & Beers 2000; Bensby, Feltzing & Lundström 2003; Soubiran, Bienaymé & Siebert 2003; Reddy, Lambert & Allende Prieto 2006; Wyse et al. 2006; Fuhrmann 2008; Ruchti et al. 2010). Using a compilation of observational data, Navarro et al. (2011) made simple cuts in the  $[\alpha/\text{Fe}]$ – $[\text{Fe}/\text{H}]$  plane, in order to separate the Milky Way’s thick and thin discs. We adopt a similar decomposition in the simulated  $[\text{O}/\text{Fe}]$ – $[\text{Fe}/\text{H}]$  plane. Bensby & Feltzing (2012) argue that the large overlap in kinematics between thick- and thin-disc populations makes classification based on age better than classification based on kinematics. The relative difficulty of ascertaining stellar ages means that abundances, in conjunction with abundance ratios, may be the best ‘proxy’. Bovy et al. (2012b) make detailed cuts in abundance space to probe thick-disc properties.

Thirdly, our study proposes more detailed categorizations of the origin of stars that comprise the different components, going beyond *accreted* versus *in situ*. In particular, we concern ourselves with whether gas which subsequently forms stars has been involved in a ‘gas-rich merger’, as well as whether it was smoothly accreted or accreted directly from proto-galaxies/satellites. This provides a more complete perspective of the relative importance of gas-rich mergers compared with smooth accretion.

In Section 2, we review our code and initial conditions, and outline the basic properties of the resulting simulation. In Section 2.2, we follow Navarro et al. (2011) and separate our (analogous) solar neighbourhood stars on the basis of their abundances, and find that such classification results in components that could reasonably be referred to as a thin disc, thick disc and halo/metal weak thick disc (MWTG), sharing some gross characteristics to those in the Milky Way. In Section 4, we trace the origin of the stars in these populations, both in terms of where they formed (in situ or *accreted*, and where in the disc they formed), their formation dispersion and the origin of the gas from which they formed. We find that thick- and thin-disc stars form in situ and that cold accretion and gas-rich mergers supply thick-disc gas. We find in Section 6 that migration also plays a role in forming the simulated thick disc. In Section 7, we discuss the consistency of these results and the fact that most disc stars form from smooth accretion and highlight the role of migration in shaping our thick-disc population.

## 2 THE SIMULATION

### 2.1 Code and initial conditions

We analyse the simulation described in B12. To quickly review, this is a cosmological ‘zoom’ simulation, derived from the initial conditions associated with galaxy g15784 from the McMaster Unbiased Galaxy Simulations (Stinson et al. 2010), using a  $25 h^{-1}$  Mpc parent cube. The virial mass of the simulated galaxy is  $M_{\text{vir}} = 1.94 \times 10^{11} M_{\odot}$ . Further detailed chemical modelling (see below) has been incorporated into the code, and the simulation re-run: the stochastic nature of our star formation recipes means that small differences exist between the current version of the simulated galaxy and the one analysed in B12, but essential properties such as rotation curve shape, star formation history (SFH), magnitude, colour and disc scalelength are not altered significantly. In B12, we showed that secular processes, largely driven by a strong bar, resulted in the formation of a bulge with  $B/T = 0.21$  at  $z = 0$ . In the current simulation, a strong bar does not form, nor does such a significant bulge. The current simulation has  $B/T = 0.12$  at  $z = 0$ .

The simulation is evolved with the smoothed particle hydrodynamics (SPH) code *GASOLINE* (Wadsley, Stadel & Quinn 2004). *GASOLINE* employs cooling based on the radiative transfer treatment within *CLOUDY* (Shen, Wadsley & Stinson 2010), including cooling due to H, He, a variety of metal lines, in the presence of an external ultraviolet radiation field. A pressure floor is added (Robertson & Kravtsov 2008), and a maximum density limit is imposed by setting a minimum SPH smoothing length,  $h_{\text{sm}}$ , to  $\frac{1}{4}$  of the gravitational softening to ensure that gas resolves the Jeans mass and does not artificially fragment. We have  $\sim 4$  million resolution elements (gas+dark matter+star) within the virial radius at  $z = 0$ , with a mean stellar particle mass of  $7300 M_{\odot}$  and a gravitational smoothing length of 155 pc.

When gas reaches cool ( $T < 10\,000$  K) temperatures in a dense ( $n_{\text{th}} > 9.3 \text{ cm}^{-3}$ ) environment, it becomes eligible to form stars. This value for  $n_{\text{th}}$  is the maximum density gas can reach using gravity. Gas is converted to stars according to the equation

$$\frac{\Delta M_{\star}}{\Delta t} = c_{\star} \frac{M_{\text{gas}}}{t_{\text{dyn}}}, \quad (1)$$

where  $\Delta M_{\star}$  is the mass of the star particle formed,  $\Delta t$  the time-step between star formation events,  $M_{\text{gas}}$  the mass of the gas particle and  $t_{\text{dyn}}$  the gas particle’s dynamical time.  $c_{\star}$  is the efficiency of star formation, in other words, the fraction of gas that will be converted into stars during  $t_{\text{dyn}}$ .

Two types of energetic feedback are considered: supernovae and stellar radiation. Supernova feedback is implemented using the blast-wave formalism described in Stinson et al. (2006) and each supernova is assumed to deposit  $10^{51}$  erg of energy into the surrounding interstellar medium (ISM). Since this gas is dense, the energy would be quickly radiated away due to the efficient cooling in SPH. For this reason, cooling is disabled for particles inside the blast region. We model the luminosity of stars using the Torres (2010) mass–luminosity relationship. These photons do not couple efficiently with the surrounding ISM (Freyer, Hensler & Yorke 2006). We thus want to couple only a small fraction of this energy to the surrounding gas in the simulation. To mimic this highly inefficient energy coupling, we first inject 10 per cent of the energy as thermal energy in the surrounding gas, and cooling is *not* turned off for this form of energy input. It is well established that such thermal energy injection is highly inefficient at the spatial and temporal resolution of the type of cosmological simulations used here (Katz 1992). This is primarily due to the characteristic cooling time-

scales in the star-forming regions being lower than the time-step of the simulations.

Metals are ejected from Type II supernovae (SNeII), SNeIa and the stellar winds driven from asymptotic giant branch stars. The ejected mass and metals are distributed to the nearest-neighbour gas particles using the smoothing kernel (Stinson et al. 2006), and we employed standard yields from the literature for SNeII (Woosley & Weaver 1995) and SNeIa (Nomoto et al. 1997). Metal diffusion is also included, such that unresolved turbulent mixing is treated as a shear-dependent diffusion term (Shen et al. 2010). This allows proximate gas particles to mix their metals. Metal cooling is calculated based on the diffused metals.

### 2.2 Evolution and properties

We emphasize again that this is not a simulated Milky Way. Our simulated galaxy is a less massive late-type galaxy, with a rotation velocity of  $\sim 140 \text{ km s}^{-1}$  and a total stellar mass within the virial radius of  $\sim 8 \times 10^9 M_{\odot}$ . The galaxy has an absolute magnitude of  $M_{B,V,I} = -19.45, -19.94, -20.71$ , and sits in the blue sequence of the colour–magnitude diagram of observed galaxies.

We plot the morphological evolution of the central galaxy in the *B* band in Fig. 1, face-on (left-hand panels) and edge-on (right-hand panels) from  $z = 2.7$  to 0 (bottom to top in the figure). Each panel is  $40 \times 40$  kpc (physical units). The major merging activity of the galaxy occurs between  $z = 2.7$  and 1.7, and we refer to this period as the ‘merger epoch’. Three significant mergers occur during this period – first, a 3:1 major merger, followed by mergers with mass ratios of 10:1 and 20:1, with the last vestiges of a merging satellite still apparent at  $z = 1.5$ . In B12, we showed that over 90 per cent of the gas which cools to the bulge region during the merger epoch is blown out to the hot halo or beyond, rather than forming bulge stars. The galaxy does not form a significant bulge during the merger epoch and has an almost pure exponential profile at  $z = 1$  (Sérsic index  $n = 1.1$ ), at which time it has a scalelength of 1.7 kpc. The scalelength of the disc component at  $z = 0$  is 2.7 kpc, as measured in the *I* band.

## 3 RESULTS

### 3.1 Components

In Fig. 2, we plot  $[\text{O}/\text{Fe}]$  versus  $[\text{Fe}/\text{H}]$  in the ‘solar annulus’, taken as the region  $7 < R_{\text{xy}} < 8$  kpc and  $|z| < 0.5$  kpc, where the disc is in the *xy* plane.<sup>1</sup> We analyse here oxygen as a representative  $\alpha$  element which is synthesized predominantly in Type II SNe, and which is an element whose synthesis is relatively well studied. An interesting feature of this plot is that there appears to be two trajectories, one stretching from  $([\text{Fe}/\text{H}], [\text{O}/\text{Fe}]) \sim (-1.1, 0.11)$  to  $([\text{Fe}/\text{H}], [\text{O}/\text{Fe}]) \sim (-0.82, 0.05)$  and the other running from  $([\text{Fe}/\text{H}], [\text{O}/\text{Fe}]) \sim (-0.85, 0.035)$  to  $([\text{Fe}/\text{H}], [\text{O}/\text{Fe}]) \sim (-0.5, -0.02)$ , offset by  $\sim 0.01$ – $0.05$  dex in  $[\text{O}/\text{Fe}]$ . We explore these trajectories by separating them into two populations simply using a straight line with equation  $[\text{O}/\text{Fe}] = -0.24 \times [\text{Fe}/\text{H}] - 0.16$  (the dashed line in Fig. 2).

The  $\sim 0.01$ – $0.05$  dex vertical offset between the two ‘tracks’ appears to be the result of the reduction in the star formation rate

<sup>1</sup> We did similar analyses for various regions between  $5 < R_{\text{xy}} < 9$  kpc and  $|z| < 2$  kpc; none of the trends discussed are dependent upon the precise region chosen as representative of the disc.

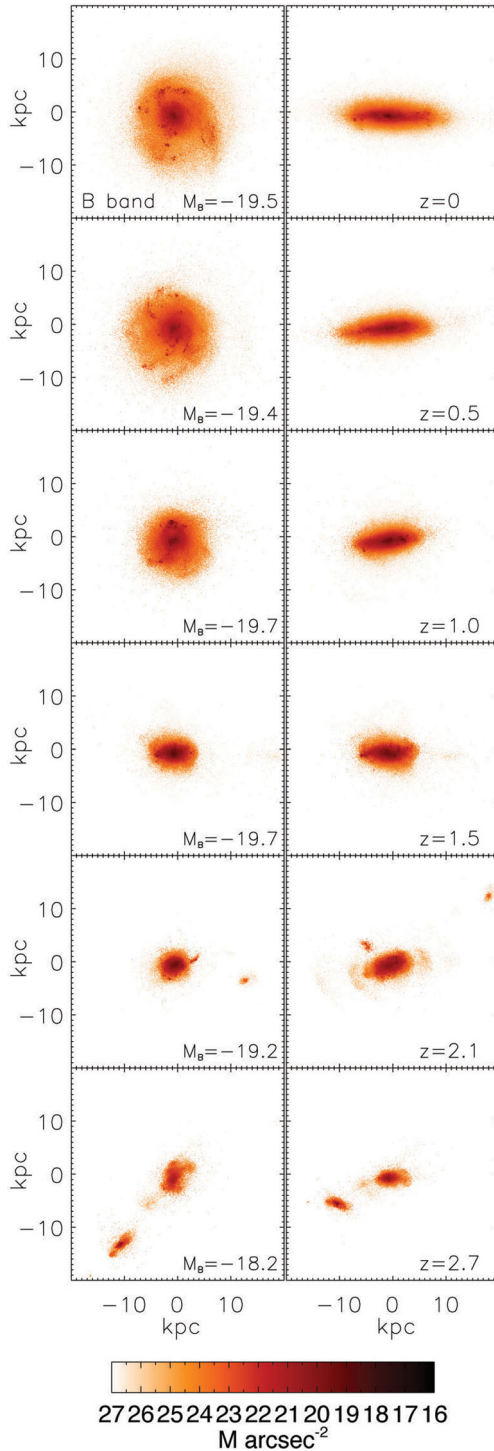


**Figure 1.** The evolution of the simulated galaxy shown in  $B$ -band surface brightness maps, as viewed both face-on (left-hand panels) and edge-on (right-hand panels). The redshifts range from  $z = 2.7$  to  $z = 0$ , and are noted in the bottom-right corner of the edge-on panels. Each panel is  $40 \times 40$  kpc (physical units). The effects of dust reprocessing, as implemented with *SUNRISE*, are included.

(SFR)  $\sim 6.6$  Gyr ago, when  $[\text{Fe}/\text{H}] \sim -0.85$  (see Figs 7 and 3). In the case of the Milky Way, the tracks are offset vertically by  $\sim 0.2$  dex, rather than the  $\sim 0.01$ – $0.05$  dex seen here. Yet the existence of these two tracks and the nature of their offset motivate us to

associate the populations with the thick (above the line) and thin (below the line) discs.

The larger offset in the Milky Way (0.2 dex) has been interpreted as indicating a hiatus in star formation in the Milky Way, along with an initiation of metal-poor gas inflow associated with the formation of the thin disc (e.g. Chiappini, Matteucci & Romano 2001; Fenner & Gibson 2003). Increased inflows of metal-poor gas were not seen  $\sim 6.6$  Gyr ago in this simulation, and we see a star formation reduction rather than hiatus. This could explain the difference with the dual infall models in the size of the offset. Further simulations with more massive galaxies will be needed to explore whether a star formation reduction coupled with the gas cycle produced in our simulation can result in larger offsets in the tracks, or whether further processes can be invoked that would lead to a hiatus in star formation. We note that Schönrich & Binney (2009) attain bimodal distributions in  $[\text{O}/\text{Fe}]$  as a consequence of their assumptions about SFRs and metal enrichment, without a star formation hiatus. We also repeat the warning provided in Schönrich & Binney (2009): it is important to bear in mind that our simulation data are a kinematically unbiased sample, while most similar observational plots are for samples that are kinematically biased in favour of thick-disc stars. In fact, Bovy et al. (2012a) show that the bimodality in  $[\alpha/\text{Fe}]$  is greatly diminished once the populations are correctly weighted.

We next analysed the properties of the two populations of stars as defined by the aforementioned linear separation. In Fig. 3, we plot the SFH of stars in the solar annulus (black line); the formation history of stars above the dashed line in Fig. 2 (the putative thick disc) is plotted in red while the stars below the dashed line in Fig. 2 (thin disc) are plotted in blue. A simple cut at the low-metallicity end of the thick-disc trajectory through this abundance space also allows us to classify stars with  $[\text{Fe}/\text{H}] < -1.3$  as belonging to the stellar halo, although we will see that this population may be better described as including an MWTG, particularly in the range  $-1.5 < [\text{Fe}/\text{H}] < -1.3$ . The SFH of halo stars is plotted in yellow in Fig. 3. The separation of the ages of stars, as selected by abundances, is clear.

The thin-disc stars are exclusively young, mostly less than 6.6 Gyr old, but with a small number of stars as old as 8.5 Gyr. The thick-disc stars are mostly older than 6.6 Gyr, and range from 5.5 to 10 Gyr. The ages of our selected halo population ranges from 9.5 to 12 Gyr. The mass of stars in the thin, thick and halo/MWTG components in this region is  $22.6$ ,  $8.9$  and  $1.3 \times 10^7 M_{\odot}$ , respectively. The dotted lines indicate times chosen for a pure age classification of the components, which will be explored alongside the metallicity cuts in the next subsection.

### 3.2 Component abundances

In Fig. 2, we show the distributions of  $[\text{Fe}/\text{H}]$  and  $[\text{O}/\text{Fe}]$  in the solar annulus stars for the thin-disc (blue line), thick-disc (red line) and halo (yellow) populations, again using abundance cuts (solid lines) and age cuts (dashed lines). This merely confirms that the selection of stars based on metallicity corresponds closely to the ages of the populations.

### 3.3 Component kinematics

In Fig. 4, we plot the distribution of the rotational velocity ( $V$ ) of the solar annulus stars for the thin-disc (blue line), thick-disc (red line) and halo (yellow) populations using abundance cuts (solid lines)

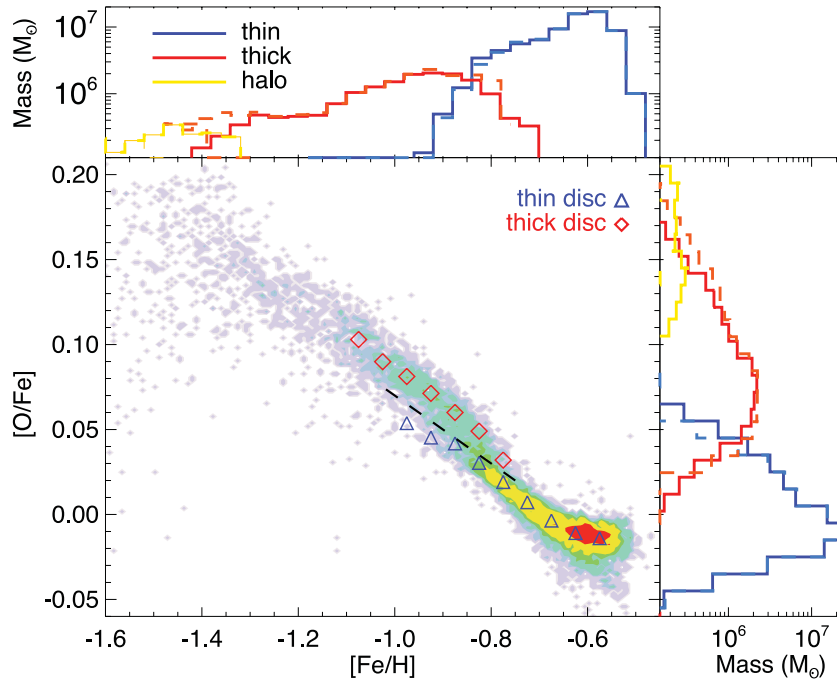


**Figure 2.**  $[O/Fe]$ – $[Fe/H]$  of simulation stars in the region  $7 < R_{xy} < 8$  kpc,  $|z| < 0.5$  kpc. Two ‘evolutionary tracks’ are evident, loosely delineated by the dashed line:  $[O/Fe] = -0.24 \times [Fe/H] - 0.16$ . This simple delineation defines what we label ‘thick’- and ‘thin’-disc populations in this work. We then overplot the means of the thick (red diamonds) and thin (blue triangles) discs  $[O/Fe]$  as a function of  $[Fe/H]$ , for the populations as defined by their ages (see the text). Above (on the right) is plotted the distribution of  $[Fe/H]$  ( $[O/Fe]$ ) in the ‘solar annulus’ for thin-disc (blue line) and thick-disc (red line) stars, based on abundances (solid) and age (dashed).

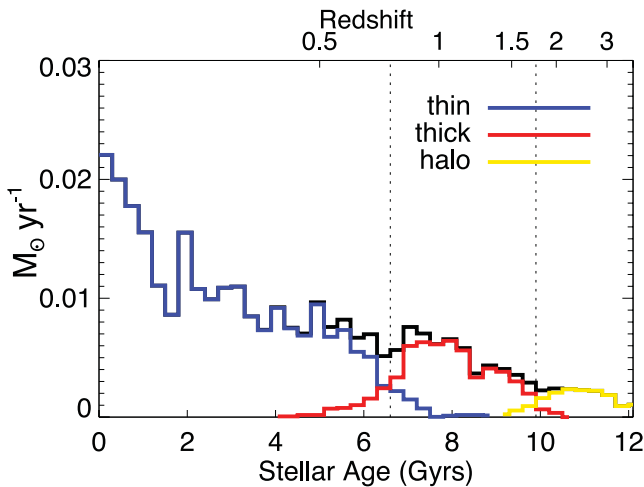


**Figure 3.** The SFH of stars in the solar annulus, defined as the region  $7 < R_{xy} < 8$  and  $|z| < 0.5$  kpc (black line). The SFH of the thin disc (blue line), thick disc (red line) and halo (yellow line), as defined by abundances in the  $[O/Fe]$ – $[Fe/H]$  plane, is overplotted.

and age cuts (dashed lines) as defined in Section 3.1. The thick disc lags the thin disc by  $\sim 25$  km  $s^{-1}$ . The  $V$  distribution of halo stars shows that there is rotation in this low-metallicity stellar population, although there is a hint of more than one population. The dispersion in  $U$  (radial velocity),  $V$  and  $W$  (the velocity perpendicular to the disc plane) of the stars in the solar annulus for the thin disc, thick disc and halo is (in km  $s^{-1}$ )  $\sigma_{U,V,W} = (41,31,25)$ ,  $(49,44,35)$  and  $(62,46,45)$ , respectively.

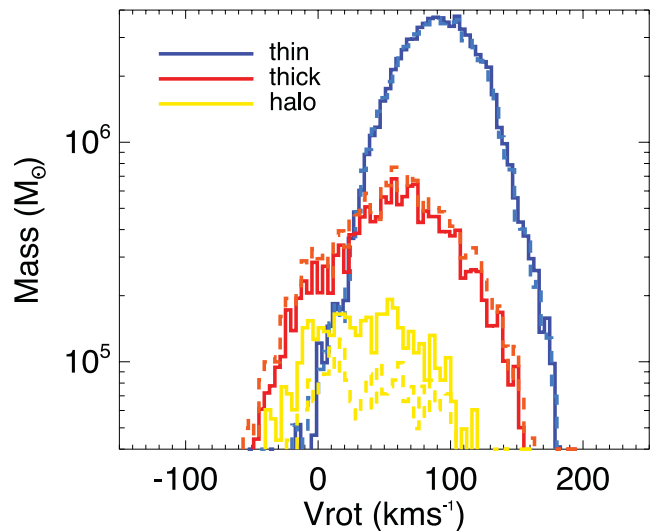


**Figure 4.** The distribution of rotational velocities in the solar annulus for the thin-disc (blue line) and thick-disc (red line) stars, based on abundances (solid) and ages (dashed). Note the log scale.

### 3.4 Evolution of velocity dispersion

The age–velocity dispersion relation for solar annulus stars is plotted in Fig. 5, showing  $\sigma_{U,V,W}$  as green diamonds, blue crosses and red asterisks, respectively. Gradual heating is apparent to a look-back time of  $\sim 11$  Gyr, more in line with the conclusions of Nordström et al. (2004) than Quillen & Garnett (2001), although this is a complex issue that we have explored earlier in the context of more massive disc simulations (House et al. 2011). In this latter work, we

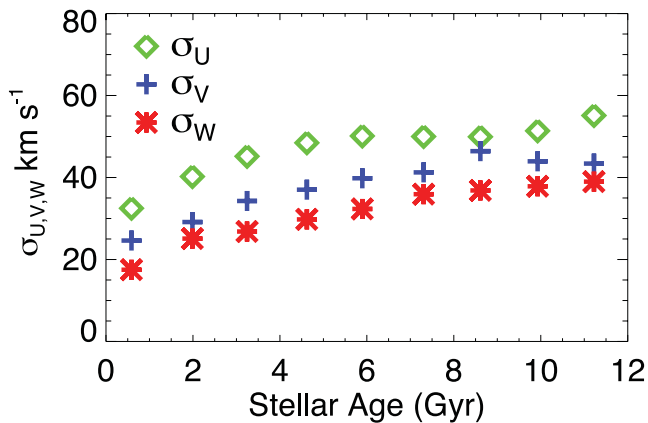


**Figure 5.** The age–velocity dispersion relation for solar annulus stars, showing  $\sigma_{U,V,W}$  as green diamonds, blue crosses and red asterisks, respectively.

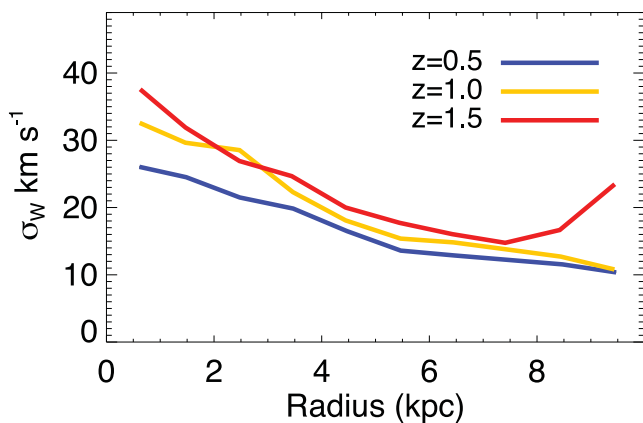


**Figure 6.**  $\sigma_W$  versus radius of young stars (age < 200 Myr) in the disc plane ( $|z| < 0.5$  kpc) at three different epochs:  $z = 1.5$  (red line);  $z = 1$  (yellow line);  $z = 0.5$  (blue line).

showed that numerical heating does not cause gradual heating that we are seeing in these simulations.

We examine the evolution of velocity dispersion in more detail in Fig. 6, where we plot  $\sigma_W$  versus radius of young stars (age < 200 Myr) at three different times, first at  $z = 1.5$  (red line), a time corresponding to the early period of thick-disc star formation, then at  $z = 1$  (yellow line) which is at the end of the thick-disc star formation and finally a later time ( $z = 0.5$  blue line) during the thin-disc formation epoch. At each epoch, we use young stars in the disc plane ( $|z| < 0.5$  kpc) of the galaxy. It is evident that the disc stars that were forming at high redshift were born kinematically hotter than those born at later times. Combined with Fig. 1, we can say that the stars forming at the end of the gas-rich merger epoch create a relatively short and kinematically hot disc structure. We note that the extent of this old disc is also reflected in the  $z = 1.5$  dispersion–radius plots, with the jump in dispersion at  $R_{xy} \sim 7.5$  kpc, while the disc extends beyond 9 kpc at  $z = 1$  (and beyond 12 kpc at  $z = 0$ ). Yet the difference in dispersion at the time of birth is not enough to explain the dispersion–age relation in Fig. 5. The dispersion–radius relation is important in this respect. We will see that old stars in the solar annulus that have large dispersions in Fig. 5 were preferentially born at lower radii, and hence with relatively high dispersion.

#### 4 ORIGIN OF THE COMPONENTS

$33.1 \times 10^7 M_\odot$  of stars are in the solar annulus as defined as the region  $7 < R_{xy} < 8$  kpc and  $|z| < 0.5$  kpc. Based on our abundance cuts,  $22.6 \times 10^7 M_\odot$  (68 per cent) are classified as thin disc,  $8.9 \times 10^7 M_\odot$  (27 per cent) as thick disc and  $1.3 \times 10^7 M_\odot$  (4 per cent) as halo/MWTD. We now trace the gas from which stars in the solar annulus were formed. We identify five categories (Table 1) for the origin of the stars, based on where they were formed and the source of the gas from which they were formed. First, stars formed in proto-galaxies *other* than the central galaxy and then accreted are classified as *stellar accretion* (ST ACC). These accreted stars comprise just 0.5 per cent of stars in the solar annulus, and all were classified as halo stars due to their abundances being  $[\text{Fe}/\text{H}] < -1.3$ . So 17 per cent of the stellar halo in the solar annulus was accreted in this manner. This would appear to be a fairly low fraction, and we have already stated that the halo as defined may include an MWTD. We make a stricter criterion and check *retrograde* halo stars, and find that still only 21 per cent are direct *stellar accretion*. We note that accreted stars have metallicities  $[\text{Fe}/\text{H}] < 1.8$ , so we finally make an even more strict criterion by limiting our sample to those with  $[\text{Fe}/\text{H}] < 1.8$  and find that 31 per cent of stars with these low metallicities are directly accreted. No disc stars (thick or thin) in our simulation have been accreted directly.

Stars forming from gas which is in proto-galaxies *other than* the central galaxy when it is accreted, but that does not form stars until *after* the accretion, are categorized as *clumpy gas accretion* (CLPY GAS ACC). 28 per cent of halo stars, 17 per cent of thick-disc stars, 10 per cent of thin-disc stars and 13 per cent of all stars in the solar annulus were formed via this mechanism.

Stars which formed from gas that was originally accreted smoothly, but form stars in the central galaxy during the ‘merger epoch’, were classified as *in situ stellar merger* (I-SU ST MGE) stars: 47 per cent of halo stars and 9 per cent of thick-disc stars are classified as due to an *in situ stellar merger*. Stars which form from gas that is originally accreted as smoothly to the central galaxy, but do not form stars until subsequent to the ‘merger epoch’, are classified as *in situ gas merger* (I-SU GAS MGE) stars: 7 per cent of halo stars, 49 per cent of thick-disc stars and 28 per cent of thin-disc stars are *in situ gas merger* stars, with such stars comprising a total of 33 per cent of all solar annulus stars. The remaining stars form from gas that is smoothly accreted to the central galaxy and are classified as being due to *smooth accretion* (SMTH ACC).

The halo component is dominated by a combination of direct stellar accretion and stars which form in the central galaxy (*in situ*)

**Table 1.** The origin of stars in the solar neighbourhood. *Stellar accretion* (ST ACC): stars accreted from merged non-central progenitors/satellites. *Clumpy Gas Accretion* (CLPY GAS ACC): gas accreted from merged non-central progenitors/satellites. *In situ Star Merger* (I-SU ST MGE): stars born in central galaxy during the merger epoch. *In situ Gas Merger* (I-SU GAS MGE): gas in the central galaxy during the merger epoch. *Smooth Accretion* (SMTH ACC): gas accreted subsequent to the merger epoch.

	MASS ( $10^7 M_\odot$ )	ST ACC (per cent)	CLPY GAS ACC (per cent)	I-SU ST MGE (per cent)	I-SU GAS MGE (per cent)	SMTH ACC (per cent)
Total	33.1	0.7	18	4.	33	44
Thin	22.6	0	16	0	28	56
Thick	8.9	0	23	9	49	19
Halo	1.3	17	28	47	7	1

prior to the end of the ‘merger epoch’ and are ‘knocked’ into the halo by the merger events. A significant number of the latter halo stars formed from gas that was originally accreted as gas from non-central progenitors. The remaining 7 per cent of the halo stars, as selected by their low metallicity, formed from gas which was in the central galaxy during the gas-rich mergers but formed stars during the turbulent period which followed the merger epoch. These stars actually have a net average rotation of  $30 \text{ km s}^{-1}$ , and may be associated better with an MWTD.

What we call ‘thick-disc stars’ are those which formed predominantly from gas involved in gas-rich mergers, with 49 per cent being in the central galaxy prior to the end of the merger epoch and 17 per cent in the smaller proto-galaxies accreted during this merger epoch. However, the thick-disc stars which form from this gas do so *subsequent* to this merger epoch, while the galaxy is ‘settling’. Only  $\sim 20$  per cent of the thick-disc stars in the simulation are formed from smoothly accreted, non-merger, gas – i.e. gas accreted to the galaxy that is not involved in merger events. No thick-disc stars are directly accreted during mergers. Our findings highlight that gas-rich mergers are a dominant process in the formation of thick-disc populations. Note that this is not at odds with studies which claim that cold flow accretion is the dominant source of a galaxy’s baryons. Rather, these studies, as well as ours, need to be interpreted carefully: baryons accreted prior to a major merger in studies of cold accretion (e.g. Kereš et al. 2005; Brooks et al. 2009) are counted as ‘smooth accretion’, which is dominated by cold flows at high redshift, and at all times that the virial mass is less than  $10^{11.5} M_{\odot}$ . Yet, significant amount of this gas which is classified as cold flow accretion can be involved in significant, and even major, gas-rich mergers subsequent to being accreted. The importance of gas-rich mergers is thus severely underestimated if these studies are superficially interpreted. Of course this goes both ways: the 49 per cent of the thick-disc stars that we have classified as ‘in situ gas mergers’ were formed from gas that first accreted to the disc region smoothly.

Thin-disc stars are dominated by smoothly accreted gas. We note that a not insignificant amount of gas that feeds the thin disc does come from gas-rich mergers. Much of this is recycled to the disc via the hot halo, after being ejected from the star-forming regions of the galaxy during starbursts. This large-scale galactic fountain process allows the recycled gas to gain angular momentum (B12) and aids in the suppression of the ubiquitous G-dwarf problem (Pilkington et al. 2012).

#### 4.1 Thick disc to thin disc transition

There is no *significant* ‘event’ occurring  $\sim 6\text{--}7$  Gyr ago that we can associate with the separation of the thin and thick discs. However, the galaxy’s SFR was relatively high  $\sim 7\text{--}10$  Gyr ago, and decreased somewhat near the time of the transition to thin-disc star formation. In Fig. 7, we plot the SFH of all stars of the simulated galaxy as the black dashed line, plotting the fraction of stars born per Gyr in bins of 0.5 Gyr. We also show the SFH of stars in the disc region ( $7 < R_{xy} < 8$  kpc and  $|z| < 0.5$  kpc, black line) and the SFH of disc stars according to different formation radii:  $3 < R_{\text{Form}} < 5$  kpc (red),  $5 < R_{\text{Form}} < 7$  kpc (light blue) and  $7 < R_{\text{Form}} < 9$  kpc (blue).  $R_{\text{Form}}$ , calculated using physical units, is the distance from the centre of the galaxy at which the star forms. This demonstrates the inside-out nature of the disc growth, which will have consequences for the abundances that we discuss below. The red line of Fig. 7 is also interesting in this respect. The stars in the solar annulus at  $z = 0$  that formed in the region  $3 < R_{\text{Form}} < 5$  kpc (the region where thick-disc

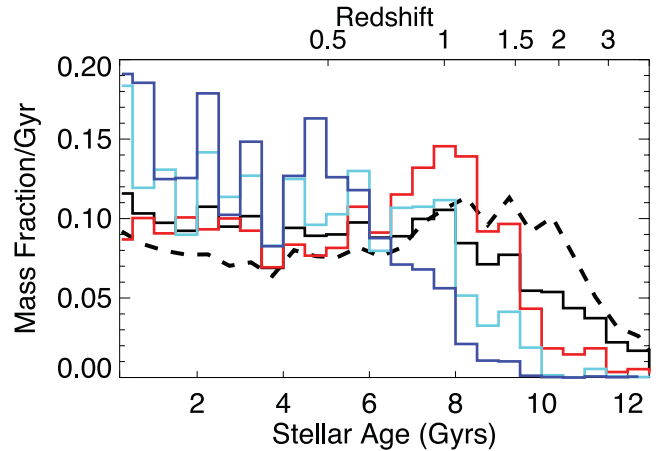


**Figure 7.** The SFH of all stars of the simulated galaxy is shown as the dashed black line, plotting the fraction of stars born per Gyr in bins of 0.5 Gyr. Overplotted is the SFH of stars in the disc (black line). We then show the SFH of disc stars according to different formation radii:  $3 < R_{\text{Form}} < 5$  (red),  $5 < R_{\text{Form}} < 7$  (light blue) and  $7 < R_{\text{Form}} < 9$  (blue).

stars predominantly formed) also have an SFR that declined around the time of transition to thin-disc star formation. Stars formed in regions further out have a more gradual build-up of star formation, meaning a longer enrichment time-scale.

## 5 STRUCTURE OF ABUNDANCE SELECTED POPULATIONS

Here we mimic Bovy et al. (2012b) and analyse the scalelength ( $h_l$ ) and scaleheight ( $h_z$ ) of stars as selected by abundances. We use our thick- and thin-disc separation as shown in our Fig. 3 to delineate the  $\alpha$ -old population as those above the dashed line, and  $\alpha$ -young as those below (using the nomenclature used in Bovy et al. 2012b).  $\alpha$ -young are then split using a simple metallicity cut<sup>2</sup> at  $[\text{Fe}/\text{H}] = -0.68$ . Metal-poor  $\alpha$ -young (MP $\alpha$ -Y) have  $[\text{Fe}/\text{H}] < -0.68$  and metal-rich  $\alpha$ -young (MR $\alpha$ -Y) have  $[\text{Fe}/\text{H}] > -0.68$ . In this section, we have extended the region of stars beyond the solar annulus in order to measure these properties, but the metallicity cuts remain valid separators of the populations. Stars taken are from the region  $4 < R_{xy} < 12$  kpc and  $0 < |z| < 4$  kpc, while scaleheights use stars in the annulus  $7 < R_{xy} < 8$  kpc and are measured out to 4 kpc. The scalelengths and scaleheights of the three populations are listed in Table 2.

As already noted, our  $\alpha$ -old (thick disc) population has a relatively short scalelength (2.31 kpc) and large scaleheight (0.9 kpc) compared to the total population which has values of 2.73 and 0.7 kpc, respectively. The features of the  $\alpha$ -young are a little less simple, and interestingly match very well the findings in Bovy et al. (2012b). First, looking at scaleheights within the solar annulus, the MP $\alpha$ -Y has a significantly larger scaleheight than the MR $\alpha$ -Y population. This simply reflects their average age, with metal-rich stars being generally younger. Yet the MP $\alpha$ -Y population has a significantly larger scalelength than the MR $\alpha$ -Y population. This is the result of the difference in chemical abundance time-scales between the inner and outer discs, relating to inside-out disc growth. The inner regions are the most chemically evolved, meaning that there remain greater relative numbers of unevolved MP $\alpha$ -Y stars further

<sup>2</sup> Results are not sensitive to this exact value.

**Table 2.** The scalelength ( $h_l$ ) and scaleheight ( $h_z$ ) of stars as selected by abundances, defining  $\alpha$ -old as those above the dashed line in Fig. 3 and  $\alpha$ -young as those below the line.  $\alpha$ -young are then split using a simple metallicity cut at  $[\text{Fe}/\text{H}] = -0.68$ . Metal-poor  $\alpha$ -young have  $[\text{Fe}/\text{H}] < -0.68$  and metal-rich  $\alpha$ -young have  $[\text{Fe}/\text{H}] > -0.68$ . Stars are from the region  $4 < R_{xy} < 12$  kpc and  $0 < |z| < 4$  kpc, while scaleheights use stars in the annulus  $7 < R_{xy} < 8$  kpc and are measured out to 4 kpc.

	Total	$\alpha$ -old	Metal-poor $\alpha$ -young	Metal-rich $\alpha$ -young
$h_l$	2.73	2.31	4.07	2.74
$h_z$	0.7	0.9	0.7	0.5

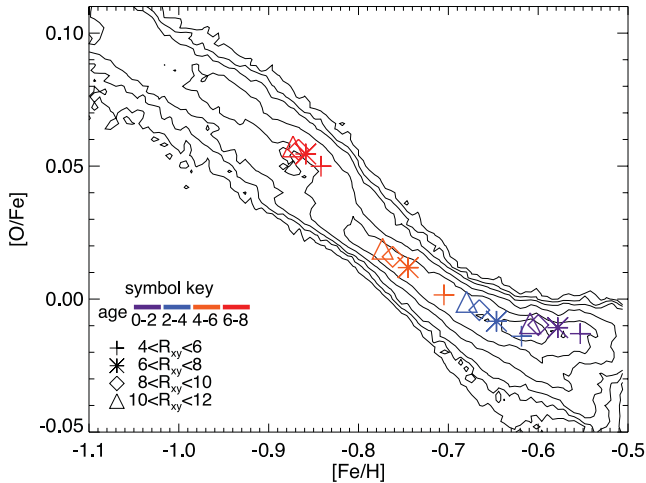


**Figure 8.** The evolution through abundance space of stars in different radial regions. The symbols represent median values of different regions in the disc, with  $R_{xy}$  (kpc) 4–6 kpc (+ sign), 6–8 kpc (star), 8–10 kpc (diamond) and 10–12 kpc (triangle). At any given time, the inner region is more chemically evolved than the outer region. This explains the longer scalelength of the less evolved metal-poor  $\alpha$ -young population (MP $\alpha$ -Y) compared with the metal-rich  $\alpha$ -young population (MR $\alpha$ -Y).

out in the disc which results in their population having a longer scalelength. Fig. 8 highlights this. The symbols represent median values of different regions in the disc, with  $R_{xy}$  4–6 kpc (+ sign), 6–8 kpc (star), 8–10 kpc (diamond) and 10–12 kpc (triangle). At any given time, the inner region is more chemically evolved than regions further out.

If migration is efficient, stars migrating to the outer disc will pollute the gas there with SN Ia, i.e. reduce the O/Fe ratio in the outer regions (see fig. 14 in Loebman et al. 2011). Thus, the degree of migration may be reflected in the observed difference in scalelength between the MP $\alpha$ -Y and MR $\alpha$ -Y populations.

## 6 MIGRATION

Migration proves to be another key process affecting the distribution of galactic components. Fig. 9 shows where stars formed that end up in the stellar annulus. The stellar annulus is demarked by the horizontal dashed lines. The dotted vertical lines show the divisions between age-defined thin-disc, thick-disc and halo populations. The mean formation radius for thick-disc stars is closer to the centre of the galaxy than the thin-disc stars. Clearly, thick-disc stars are born closer to the centre of the galaxy than the later forming thin-disc stars. We do not further examine the mode of migration here – i.e. we

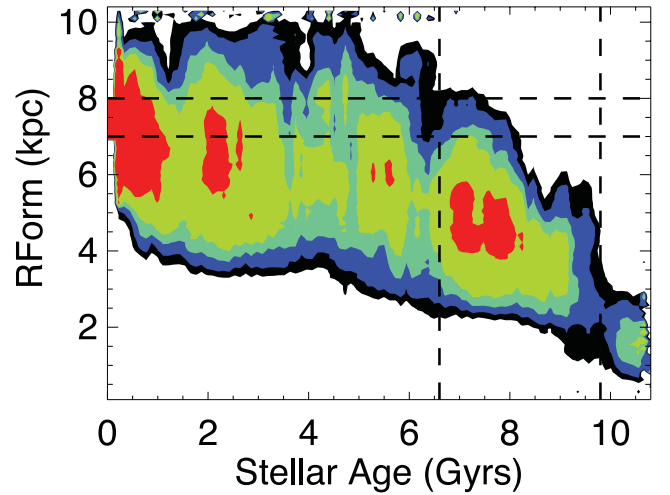


**Figure 9.** The evolution of the distribution of formation radii for stars that end up in the solar annulus:  $7 < R_{xy} < 8$ ,  $|z| < 0.5$ .

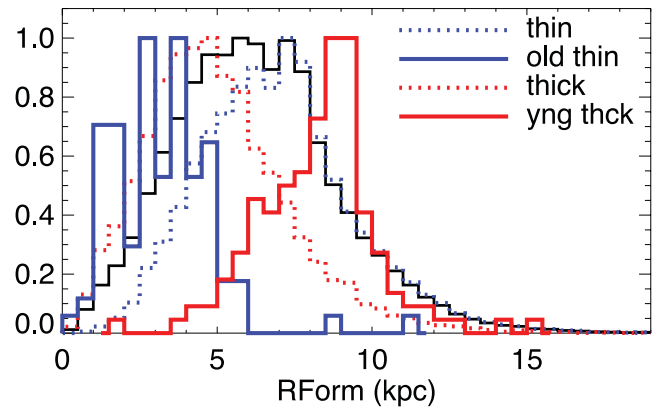


**Figure 10.** The thin black line shows the distribution of radii of star formation of solar annulus stars, with the distribution of thin (blue dotted) and thick (red dotted) overplotted. The blue and red lines show the extremely old (age  $> 7.8$  Gyr) thin- and young (age  $< 5.2$  Gyr) thick-disc stars.

do not distinguish the contributions of churning, blurring, scattering from the bar, or co-rotation scattering in this study. Briefly, we can compare our plot and figs 3 and 5 of Loebman et al. (2011): the degree of migration is larger than in their fig. 5, the case where little co-rotation scattering occurs due to weak spiral structure, but is lower than in fig. 3, where significant co-rotation scattering occurs.

Fig. 10 shows a component by component analysis of migration. For this analysis, we revert to selecting the components based on metallicity. The solid black line shows the total distribution of formation radius. The red line shows the thick disc and the blue line shows the thin-disc distributions.

We separate outlier stars out of the thick- and thin-disc populations, to try to understand why some young stars share abundances with the thick-disc population, while some old stars share abundances with the thin disc. The young (age  $< 5.2$  Gyr) thick-disc population is shown as the dotted red line, and the old (age  $> 7.8$  Gyr) thin-disc population is shown as the dotted blue line. Clearly, old thin-disc stars were born closer to the centre of the galaxy than the general disc population, and at even smaller radii than the thick-disc population. This is explained by the fact that the inner region is more chemically evolved because the disc grows inside-out (see also Pilkington et al. 2012), so the  $[\alpha/\text{Fe}]$  ratio becomes lower at an

earlier time in the innermost region than in regions further out. Thus, old stars born in this inner region have thin-disc abundances. Contrastingly, young thick-disc stars (based on abundances) migrated from outer regions, which were relatively unevolved chemically. This is similar to findings in the models of Schönrich & Binney (2009).

We also examine the dispersion of stars in these populations, and find that for the old thin disc  $\sigma_w = 31 \text{ km s}^{-1}$ , comparable to other stars of similar age.  $\sigma_w$  of young thick-disc stars (migrated from outer regions) is  $\sim 36 \text{ km s}^{-1}$ , similar to the rest of the thick-disc population. We compare with young stars that have migrated from the inner regions ( $R_{\text{form}} < 5 \text{ kpc}$  – i.e. the region from which thick-disc stars predominantly migrated) and find  $\sigma_w = 25 \text{ km s}^{-1}$ . This indicates that migration alone will not build a thick disc in our simulation, and highlights the importance that the original old disc is born relatively hot, as shown in Fig. 6.

## 7 DISCUSSION

### 7.1 Milky Way comparisons

We do not want to overemphasize any comparison to the Milky Way that can be drawn from our study, and remind the reader again that the simulated galaxy has significantly lower mass, and will have a different merger history. We do want to emphasize that this simulated galaxy has a low-mass, low-metallicity, stellar halo. The majority of previous simulations that have analysed the origins of stellar components have had overly massive spheroids (e.g. Abadi et al. 2003; Zolotov et al. 2009; Kobayashi & Nakasato 2011; Tissera et al. 2011) (from the accretion of an excess of stars) and suffered from an inability to match the empirical stellar mass–halo mass relation (e.g. Piontek & Steinmetz 2011). The mass and metallicity of the stellar halo provide strict constraints on galaxy formation simulations (Brook et al. 2004a; Okamoto et al. 2005). We showed that we were able to separate thin- and thick-disc stars based on abundances (and age), in a similar manner to Navarro et al. (2011) for the Milky Way. The qualitative similarities between the simulation and the Milky Way of having two tracks for the two populations through the [O/Fe], [Fe/H] plane are indeed interesting, and we attribute the change from thick-disc to thin-disc star formation to a drop in the SFR, associated with the end of the rapid gas accretion phase (Kereš et al. 2005) and the end of the gas-rich merger epoch. The *degree* of separation of these tracks may be an instructive diagnostic: the two tracks in the simulation are closer together (separated by  $\sim 0.01$ – $0.05$  dex in [O/Fe]) than the Milky Way tracks (separated by  $\sim 0.2$  dex in [O/Fe]; Bensby et al. 2005; Reddy et al. 2006; Fuhrmann 2008), which has been interpreted by chemical evolution models as indicating that the Milky Way experienced a *hiatus* in star formation (e.g. Chiappini et al. 2001; Fenner & Gibson 2003). Schönrich & Binney (2009) attain bimodal distributions in [O/Fe] as a consequence of their assumptions about SFRs and metal enrichment, without a star formation hiatus (their star formation is assumed to exponentially decay). Yet we remind the reader that the degree of offset in the observed relations in Milky Way may, at least partially, be due to the kinematic selection which is biased towards thick-disc stars.

### 7.2 Components

We have made a component analysis of a simulated disc galaxy. We categorize stars as belonging to the thin disc, thick disc and halo by simple cuts in abundances of [O/Fe] and [Fe/H] in a manner similar to that done for observed stars in Navarro et al. (2011). In qualitative sense, the properties of the components are reasonable analogues

of the Milky Way components, in terms of velocity dispersion, rotation velocities and metallicity. We trace the origin of gas from which stars in the different components form.

*Halo.* In the solar neighbourhood, most stars form in situ but are knocked into the halo during the merger epoch. This is quantitatively higher than the fraction of in situ halo stars as suggested in Zolotov et al. (2009), who predicted that a significant fraction of halo stars are formed in situ, but found that accretion remains the dominant source of halo stars. We attribute this difference to the low stellar mass fractions of the accreted proto-galaxies/satellites in our simulations, which better match empirical relations between stellar and halo mass (Brook et al. 2012b). This also results in the low-mass, low-metallicity halo of the current simulation. By contrast, using physical recipes similar to those used in Zolotov et al. (2009) has been shown to result in significantly too many stars compared to the empirical relation between stellar and total halo masses (Sawala et al. 2011) in low-mass galaxies, exaggerating the number of accreted stars and resulting in spheroids that are more massive and more metal rich than those observed in the Milky Way. In our simulated galaxy there is still a significant fraction ( $\sim 17$ – $31$  per cent) of local halo stars that are directly accreted from smaller proto-galaxies/satellites.

*Thick disc.* Thick-disc stars all form in situ. Again this is in contrast to numerous studies of simulated Milky Way mass galaxies, which claim significant numbers of accreted thick-disc stars (e.g. Abadi et al. 2003; Kobayashi & Nakasato 2011; Tissera et al. 2011). We note that those previous studies have stellar spheroids that are significantly more massive than those observed in the Milky Way. Significant numbers of accreted thick-disc stars have not been shown to form without corresponding massive spheroids also being accreted (e.g. Abadi, Navarro & Steinmetz 2006; Tissera et al. 2011). In our simulated galaxy, around 77 per cent of thick-disc stars form from gas that is directly accreted to the central galaxy, while 23 per cent is accreted as clumpy gas – i.e. gas which is part of an accreted proto-galaxy/satellite. Yet, most of the thick-disc-forming gas is accreted prior to the end of the ‘merger epoch’, meaning that most ( $\sim 80$  per cent) of thick disc gas is involved in a gas-rich merger at high redshift. Thick-disc stars form as the gas settles into a disc at the end of the merger epoch. The thick disc has a relatively short radial scalelength and is kinematically ‘hot’ as it forms.

*Thin disc.* The thin-disc stars form primarily from gas that is smoothly accreted to the central galaxy subsequent to the end of the merger epoch. A significant number of thin-disc stars form from gas accreted during the merger epoch, either directly to the central galaxy or as part of an accreted proto-galaxy, which is cycled through the galaxy’s hot corona in a large-scale galactic fountain (see B12).

*Transitions.* In our simulation, the end of the merger epoch marks the transition from halo-star formation to thick-disc star formation. No ‘event’ marks the transition from thick to thin disc in our simulation. We do note that the thick-disc formation time is longer in our simulation than most estimates of the Milky Way thick disc [ $\sim 3.5$  Gyr compared to 1–2 Gyr (e.g. Fuhrmann 2008; Smiljanic et al. 2009), although Bensby et al. (2007) claim a time-scale of 3 Gyr]. This may be due to the lower mass of our simulated galaxy, which would result in a longer time for the thick disc to settle down. This would be consistent with observations which indicate that thick discs are more prominent in lower mass disc galaxies (Yoachim & Dalcanton 2006). Alternatively, it may of course be a problem with our model.

*Inside-out chemical evolution.* The thick disc (with an  $\alpha$ -old population, i.e. stars above the dashed line in Fig. 3) has a scalelength of 2.31 kpc at  $z = 0$ . The inside-out growth of the thin disc ( $\alpha$ -young stars, below the dashed line in Fig. 3) results in differences in chemical abundance time-scales between the inner and outer discs. The inner regions are the most chemically evolved, meaning that there remain greater relative numbers of unevolved metal-poor  $\alpha$ -young stars further out in the disc, which results in the population having a longer scalelength (4.07 kpc) compared to the metal-rich  $\alpha$ -young stars (2.74 kpc).

*Migration.* The stars classified as thick disc in our model preferentially were born closer to the centre of the galaxy, and migrated to the solar neighbourhood. Our model is fully cosmological, yet it is chosen to have a quiescent merger period at late ( $z < 1.5$ ) times. At these times, it thus resembles the models of Loebman et al. (2011), and it is interesting that their collapse model also initially forms a relatively short, kinematically hot, disc at high redshift before the thin-disc formation begins. The dissipative nature of the gas-rich merger epoch in our case and the collapse of a rotating sphere in their case (and in the study of Samland & Gerhard 2003) have resulted in information of the early differences between the models being lost, at least in kinematics alone. Loebman et al. (2011) also found that simple cuts in abundance space could result in populations with thick- and thin-disc properties. Detailed chemical ‘fingerprints’ that will become available in surveys such as GALactic Archaeology with HERMES (GALAH) may combine with GAIA kinematic data to unravel star formation sites (Freeman & Bland-Hawthorn 2002; De Silva et al. 2006). We also note that the initial conditions imposed in the dynamical model of Schönrich & Binney (2009) consist of a relatively hot and short disc. Our simulations suggest that migration is part of the story of thick-disc formation, but not necessarily to the exclusion of other theories. The recent paper of Liu & van de Ven (2012) finds evidence for both migration and gas-rich mergers in the relationships between eccentricities and abundances.

## ACKNOWLEDGMENTS

BKG and CBB acknowledge the support of the UK’s Science & Technology Facilities Council (ST/F002432/1 & ST/H00260X/1). BKG and KP acknowledge the generous visitor support provided by Saint Mary’s University and Monash University. TRQ was supported by NSF Grant AST-0908499. We thank the DEISA consortium, co-funded through EU FP6 project RI-031513 and the FP7 project RI-222919, for support within the DEISA Extreme Computing Initiative, the UK’s National Cosmology Supercomputer (COSMOS) and the University of Central Lancashire’s High Performance Computing Facility. CBB and AVM acknowledge funding by Sonderforschungsbereich SFB 881 ‘The Milky Way System’ (sub-project A1) of the German Research Foundation (DFG).

## REFERENCES

Abadi M. G., Navarro J. F., Steinmetz M., Eke V. R., 2003, *ApJ*, 597, 21  
 Abadi M. G., Navarro J. F., Steinmetz M., 2006, *MNRAS*, 365, 747  
 Agertz O., Teyssier R., Moore B., 2009, *MNRAS*, 397, L64  
 Assmann P., Fellhauer M., Kroupa P., Bruens R. C., Smith R., 2011, *MNRAS*, 415, 1280A  
 Bensby T., Feltzing S., 2012, *European Phys. J. Web Conf.*, 19, 4001  
 Bekki K., Tsujimoto T., 2011, *MNRAS*, 416, L60  
 Bensby T., Feltzing S., Lundström I., 2003, *A&A*, 410, 527  
 Bensby T., Feltzing S., Lundström I., Ilyin I., 2005, *A&A*, 433, 185  
 Bensby T., Zenn A. R., Oey M. S., Feltzing S., 2007, *ApJ*, 663, L13

Bournaud F., Elmegreen B. G., Elmegreen D. M., 2007, *ApJ*, 670, 237  
 Bovy J., Rix H.-W., Hogg D. W., 2012a, *ApJ*, 751, 131  
 Bovy J., Rix H.-W., Liu C., Hogg D. W., Beers T. C., Lee Y. S., 2012b, *ApJ*, 753, 148  
 Brook C. B., Kawata D., Gibson B. K., Flynn C., 2004a, *MNRAS*, 349, 52  
 Brook C. B., Kawata D., Gibson B. K., Freeman K. C., 2004b, *ApJ*, 612, 894  
 Brook C. B., Stinson G., Gibson B. K., Roškar R., Wadsley J., Quinn T., 2012a, *MNRAS*, 419, 771 (B12)  
 Brook C. B., Stinson G., Gibson B. K., Wadsley J., Quinn T., 2012b, *MNRAS*, 424, 1275  
 Brooks A. M., Governato F., Quinn T., Brook C. B., Wadsley J., 2009, *ApJ*, 694, 396  
 Ceverino D., Dekel A., Bournaud F., 2010, *MNRAS*, 404, 2151  
 Chiappini C., Matteucci F., Romano D., 2001, *ApJ*, 554, 1044  
 Chiba M., Beers T. C., 2000, *AJ*, 119, 2843  
 Dalcanton J. J., Bernstein R. A., 2002, *AJ*, 124, 1328  
 De Silva G. M., Sneden C., Paulson D. B., Asplund M., Bland-Hawthorn J., Bessell M. S., Freeman K. C., 2006, *AJ*, 131, 455  
 Doménech-Moral M., Martínez-Serrano F. J., Domínguez-Tenreiro R., Serna A., 2012, *MNRAS*, 421, 2510  
 Fenner Y., Gibson B. K., 2003, *PASA*, 20, 189  
 Freeman K., Bland-Hawthorn J., 2002, *ARA&A*, 40, 487  
 Freyer T., Hensler G., Yorke H. W., 2006, *ApJ*, 638, 262  
 Fuhrmann K., 1998, *A&A*, 338, 161  
 Fuhrmann K., 2008, *MNRAS*, 384, 173  
 Gilmore G., Reid N., 1983, *MNRAS*, 202, 1025  
 Governato F., Willman B., Mayer L., Brooks A., Stinson G., Valenzuela O., Wadsley J., Quinn T., 2007, *MNRAS*, 374, 1479  
 Guedes J., Callegari S., Madau P., Mayer L., 2011, *ApJ*, 742, 76  
 Hammer F., Puech M., Chemin L., Flores H., Lehnert M. D., 2007, *ApJ*, 662, 322  
 Hayashi H., Chiba M., 2006, *PASJ*, 58, 835  
 House E. L. et al., 2011, *MNRAS*, 415, 2652  
 Ivezić Ž. et al., 2008, *ApJ*, 684, 287  
 Jurić M. et al., 2008, *ApJ*, 673, 864  
 Katz N., 1992, *ApJ*, 391, 502  
 Kazantzidis S., Bullock J. S., Zentner A. R., Kravtsov A. V., Moustakas L. A., 2008, *ApJ*, 688, 254  
 Kereš D., Katz N., Weinberg D. H., Davé R., 2005, *MNRAS*, 363, 2  
 Kobayashi C., Nakasato N., 2011, *ApJ*, 729, 16  
 Kroupa P., 2002, *MNRAS*, 330, 707  
 Liu C., van de Ven G., 2012, submitted  
 Loebman S. R., Roškar R., Debattista V. P., Ivezić Ž., Quinn T. R., Wadsley J., 2011, *ApJ*, 737, 8  
 Majewski S. R., 1993, *ARA&A*, 31, 575  
 Martig M., Bournaud F., Croton D. J., Dekel A., Teyssier R., 2012, *ApJ*, in press  
 Navarro J. F., Abadi M. G., Venn K. A., Freeman K. C., Anguiano B., 2011, *MNRAS*, 412, 1203  
 Noguchi M., 1999, *ApJ*, 514, 77  
 Nomoto K., Iwamoto K., Nakasato N., Thielemann F.-K., Brachwitz F., Tsujimoto T., Kubo Y., Kishimoto N., 1997, *Nucl. Phys. A*, 621, 467  
 Nordström B. et al., 2004, *A&A*, 418, 989  
 Okamoto T., Eke V. R., Frenk C. S., Jenkins A., 2005, *MNRAS*, 363, 1299  
 Pilkington K. et al., 2012, *MNRAS*, in press  
 Piontek F., Steinmetz M., 2011, *MNRAS*, 410, 2625  
 Qu Y., Di Matteo P., Lehnert M. D., van Driel W., 2011, *A&A*, 530, A10  
 Quillen A. C., Garnett D. R., 2001, in Funes J. G., Corsini E. M., eds, *ASP Conf. Ser. Vol. 230, Galaxy Disks and Disk Galaxies*. Astron. Soc. Pac., San Francisco, p. 87  
 Quinn P. J., Hernquist L., Fullagar D. P., 1993, *ApJ*, 403, 74  
 Reddy B. E., Lambert D. L., Allende Prieto C., 2006, *MNRAS*, 367, 1329  
 Robertson B. E., Kravtsov A. V., 2008, *ApJ*, 680, 1083  
 Ruchti G. R. et al., 2010, *ApJ*, 721, L92  
 Sales L. V., Navarro J. F., Theuns T., Schaye J., White S. D. M., Frenk C. S., Crain R. A., Dalla Vecchia C., 2012, *MNRAS*, 423, 1544

- Samland M., Gerhard O. E., 2003, *A&A*, 399, 961  
Sawala T., Guo Q., Scannapieco C., Jenkins A., White S., 2011, *MNRAS*, 413, 659  
Scannapieco C., Gadotti D. A., Jonsson P., White S. D. M., 2010, *MNRAS*, 407, L41  
Scannapieco C. et al., 2012, *MNRAS*, 423, 1726  
Schönrich R., Binney J., 2009, *MNRAS*, 399, 1145  
Shen S., Wadsley J., Stinson G., 2010, *MNRAS*, 407, 1581  
Smiljanic R., Pasquini L., Bonifacio P., Galli D., Gratton R. G., Randich S., Wolff B., 2009, *A&A*, 499, 103  
Soubiran C., Bienaymé O., Siebert A., 2003, *A&A*, 398, 141  
Stinson G., Seth A., Katz N., Wadsley J., Governato F., Quinn T., 2006, *MNRAS*, 373, 1074  
Stinson G. S., Bailin J., Couchman H., Wadsley J., Shen S., Nickerson S., Brook C., Quinn T., 2010, *MNRAS*, 408, 812  
Tissera P. B., White S. D. M., Scannapieco C., 2011, *MNRAS*, 2002  
Torres G., 2010, *AJ*, 140, 1158  
Villalobos Á., Helmi A., 2008, *MNRAS*, 391, 1806  
Wadsley J. W., Stadel J., Quinn T., 2004, *New Astron.*, 9, 137  
Woosley S. E., Weaver T. A., 1995, *ApJS*, 101, 181  
Wyse R. F. G., Gilmore G., Norris J. E., Wilkinson M. I., Kley J. T., Koch A., Evans N. W., Grebel E. K., 2006, *ApJ*, 639, L13  
Yoachim P., Dalcanton J. J., 2005, *ApJ*, 624, 701  
Yoachim P., Dalcanton J. J., 2006, *AJ*, 131, 226  
Zolotov A. et al., 2009, *MNRAS*, 347, 556

This paper has been typeset from a  $\text{\TeX}/\text{\LaTeX}$  file prepared by the author.

Copyright of Monthly Notices of the Royal Astronomical Society is the property of Wiley-Blackwell and its content may not be copied or emailed to multiple sites or posted to a listserv without the copyright holder's express written permission. However, users may print, download, or email articles for individual use.